

A Transient ‘Changing-Look’ AGN Resolved on Month Timescales From First-Year SDSS-V Data

GRISHA ZELTYN ¹, BENNY TRAKHTENBROT ¹, MICHAEL ERACLEOUS ², JESSIE RUNNOE ³, JONATHAN R. TRUMP ⁴, JONATHAN STERN ¹,
YUE SHEN ^{5,6}, LORENA HERNANDEZ-GARCIA ^{7,8}, FRANZ E. BAUER ^{9,7,10}, QIAN YANG ^{5,11}, TOM DWELLY ¹², CLAUDIO RICCI ^{13,14},
PAUL GREEN ¹¹, SCOTT F. ANDERSON ¹⁵, ROBERTO J. ASSEF ¹³, MURYEL GUOLO ¹⁶, CHELSEA MACLEOD ¹⁷, MEGAN C. DAVIS ⁴,
LOGAN FRIES ⁴, SUVI GEZARI ¹⁸, NORMAN A. GROGIN ¹⁸, DAVID HOMAN, ¹⁹ ANTON M. KOEKEMOER ¹⁸, MIRKO KRUMPE, ¹⁹
STEPHANIE LA MASSA ¹⁸, XIN LIU ^{5,6}, ANDREA MERLONI ²⁰, MARY LOLI MARTINEZ ALDAMA ^{21,22}, DONALD P. SCHNEIDER ²,
MATTHEW J. TEMPLE ¹³, JOEL R. BROWNSTEIN ²³, HECTOR IBARRA-MEDEL ^{5,24}, JAMISON BURKE ^{25,26} AND CRAIG PELLEGRINO ^{25,26}

¹*School of Physics and Astronomy, Tel Aviv University, Tel Aviv 69978, Israel*

²*Department of Astronomy & Astrophysics and Institute for Gravitation and the Cosmos, The Pennsylvania State University, 525 Davey Lab, University Park, PA 16802, USA*

³*Department of Physics and Astronomy, Vanderbilt University, Nashville, TN 37235, USA*

⁴*Department of Physics, 196 Auditorium Road, Unit 3046, University of Connecticut, Storrs, CT 06269, USA*

⁵*Department of Astronomy, University of Illinois at Urbana-Champaign, Urbana, IL 61801, USA*

⁶*National Center for Supercomputing Applications, University of Illinois at Urbana-Champaign, Urbana, IL 61801, USA*

⁷*Millennium Institute of Astrophysics (MAS), Nuncio Monseñor Sótero Sanz 100, Providencia, Santiago, Chile*

⁸*Instituto de Física y Astronomía, Facultad de Ciencias, Universidad de Valparaíso, Gran Bretaña 1111, Valparaíso, Chile*

⁹*Instituto de Astrofísica and Centro de Astroingeniería, Facultad de Física, Pontificia Universidad Católica de Chile, Casilla 306, Santiago 22, Chile*

¹⁰*Space Science Institute, 4750 Walnut Street, Suite 205, Boulder, CO 80301, USA*

¹¹*Center for Astrophysics | Harvard & Smithsonian, 60 Garden Street, Cambridge, MA 02138, USA*

¹²*Max-Planck-Institut für extraterrestrische Physik, Giessenbachstraße, 85748 Garching, Germany*

¹³*Núcleo de Astronomía de la Facultad de Ingeniería, Universidad Diego Portales, Av. Ejército Libertador 441, Santiago, Chile*

¹⁴*Kavli Institute for Astronomy and Astrophysics, Peking University, Beijing 100871, People’s Republic of China*

¹⁵*Astronomy Department, University of Washington, Box 351580, Seattle, WA 98195, USA*

¹⁶*Department of Physics and Astronomy, Johns Hopkins University, 3400 N. Charles St., Baltimore MD 21218, USA*

¹⁷*BlackSky, 1505 Westlake Ave North #600, Seattle, WA 98109, USA*

¹⁸*Space Telescope Science Institute, 3700 San Martin Dr., Baltimore, MD 21218, USA*

¹⁹*Leibniz-Institut für Astrophysik Potsdam An der Sternwarte 16, 14482 Potsdam, Germany*

²⁰*Max-Planck-Institut für Extraterrestrische Physik, Giessenbachstraße, 85748 Garching, Germany*

²¹*Instituto de Física y Astronomía, Facultad de Ciencias, Universidad de Valparaíso, Gran Bretaña 1111, Valparaíso, Chile*

²²*Departamento de Astronomía, Universidad de Chile, Casilla 36D, Santiago, Chile*

²³*Department of Physics and Astronomy, University of Utah, 115 S. 1400 E., Salt Lake City, UT 84112, USA*

²⁴*Instituto de Astronomía y Ciencias Planetarias, Universidad de Atacama, Copayapu 485, Copiapó, Chile*

²⁵*Las Cumbres Observatory, 6740 Cortona Dr, Suite 102, Goleta, CA 93117-5575, USA*

²⁶*Department of Physics, University of California, Santa Barbara, CA 93106-9530, USA*

(Received August 15, 2022; Revised October 13, 2022; Accepted TBD)

Submitted to ApJL

ABSTRACT

We report the discovery of a new ‘changing-look’ active galactic nucleus (CLAGN) event, in the quasar SDSS J162829.17+432948.5 at $z = 0.2603$, identified through repeat spectroscopy from the fifth Sloan Digital Sky Survey (SDSS-V). Optical photometry taken during 2020-2021 shows a dramatic dimming of $\Delta g \approx 1$ mag, followed by a rapid recovery on a timescale of several months, with the $\lesssim 2$ month period of rebrightening captured in new SDSS-V and Las Cumbres Observatory spectroscopy. This is one of the fastest CLAGN transitions observed to date. Archival observations suggest that the object experienced a much more gradual dimming over the period of 2011-2013. Our spectroscopy shows that the photometric changes were accompanied by dramatic

variations in the quasar-like continuum and broad-line emission. The excellent agreement between the pre- and post-dip photometric and spectroscopic appearances of the source, as well as the fact that the dimmest spectra can be reproduced by applying a single extinction law to the brighter spectral states, favor a variable line-of-sight obscuration as the driver of the observed transitions. Such an interpretation faces several theoretical challenges, and thus an alternative accretion-driven scenario cannot be excluded. The recent events observed in this quasar highlight the importance of spectroscopic monitoring of large AGN samples on weeks-to-months timescales, which the SDSS-V is designed to achieve.

Keywords: Supermassive black holes (1663), Quasars (1319), Active galactic nuclei (16), Transient sources (1861)

1. INTRODUCTION

In recent years, optical time-domain photometric and spectroscopic wide-area surveys have revealed a multitude of highly variable active galactic nuclei (AGNs). Among those, ‘changing-look’ AGNs (CLAGNs hereafter) identified in the rest-frame UV-optical regime are events that show significant changes of the blue continuum and/or broad emission lines (BELs) that are typical of unobscured AGNs, often resulting in a transition between AGN-dominated and host-dominated spectral appearances.¹ Over the past decade, many such transitions have been discovered among highly luminous AGNs (i.e., quasars), starting from a few prototypical cases (e.g., LaMassa et al. 2015; Runnoe et al. 2016), followed by more sizable samples (e.g., Yang et al. 2018; MacLeod et al. 2019; Green et al. 2022). The nature of the surveys used to identify these events means that the extreme variability is typically traced over timescales of years. To date, only a few examples clearly show shorter timescale *spectral* transitions in the UV-optical regime (Guo et al. 2016; Trakhtenbrot et al. 2019; Ross et al. 2020). In several more cases, photometric monitoring programs imply that spectral transitions have in fact occurred over timescales of <1 year (e.g., Gezari et al. 2017; Yang et al. 2018; Frederick et al. 2019; Yan et al. 2019; Green et al. 2022).

Identifying the physical mechanisms that drive the extreme variability observed in CLAGNs can provide information about the structure and physics of the accretion flow, broad-line region (BLR) and other key AGN components, and yield insights into intermittent super-massive black hole (SMBH) growth. The mechanisms driving UV-optical CLAGN transitions, however, remain unclear, with most studies favoring explanations related to changes in the (ionizing) continuum radiation power due to variations in the accretion flow (e.g., LaMassa et al. 2015; Ruan et al. 2016; Runnoe et al. 2016; Sheng et al. 2017; Rumbaugh et al. 2018; Stern et al. 2018; Trakhtenbrot et al. 2019; Guolo et al. 2021). Alternatively,

some of the spectral transitions could result from changes in obscuring dust/gas along our line of sight (l.o.s.). Many studies of extremely variable AGNs identified in the X-rays have shown decisive evidence for variable obscuration of the central engines of some AGNs (e.g., Risaliti et al. 2005; Maiolino et al. 2010; Markowitz et al. 2014; Hernández-García et al. 2017; Liu et al. 2022, and references therein). In addition, variations to the l.o.s. obscuration of the continuum source and the BLR have been inferred from the variable optical spectra of a few Seyfert 1.8 and 1.9 galaxies (e.g., Goodrich 1995, and references therein).

In this letter we report a newly discovered CLAGN, SDSS J162829.17+432948.5 (hereafter J1628+4329), which displays recurring dramatic spectral changes over relatively short timescales, as well as transitions between seemingly distinct spectral states. After describing the observations and spectral decomposition methods (Section 2), we discuss several possible physical interpretations of the observed changes and conclude that the data may be better explained by variable obscuration (Section 3). These observations may offer the best evidence to date for variable obscuration driving a CLAGN transition in a luminous quasar, and, more generally, one of the fastest CLAGN transitions traced in both photometry and spectroscopy. A summary of our results is presented in Section 4.

Throughout this work, we adopt a flat Λ cold dark matter cosmology with $H_0 = 70 \text{ km s}^{-1} \text{ Mpc}^{-1}$ and $\Omega_m = 0.3$.

2. OBSERVATIONS AND ANALYSIS

2.1. Multi-epoch optical spectroscopy

Our key observational dataset is multi-epoch medium-resolution optical spectroscopy of the AGN J1628+4329, at $z = 0.2603$ (at a luminosity distance of $\approx 1320 \text{ Mpc}$ and an angular scale of $\approx 4 \text{ kpc}''$), collected over a span of over two decades. The spectra used for our main analysis are shown in Fig. 1; details about the observations are provided in Table 1.

The first spectrum was obtained in May 2001 as part of the legacy Sloan Digital Sky Survey (SDSS; York et al. 2000). This spectrum shows a blue continuum and broad Balmer emission lines typical of unobscured AGNs, with a quasar-like continuum luminosity ($\log(\lambda L_\lambda[5100 \text{ \AA}]/\text{erg s}^{-1}) \approx 44$;

¹ Throughout this Letter, we use the term CLAGN to refer to *all* AGNs that show such spectral transitions, regardless of the physical mechanisms driving these changes.

see Section 2.3) In what follows, we refer to this 2001 spectrum as the “bright state”.

The second spectrum was obtained following the identification of J1628+4329 as a highly variable source based on SDSS and Pan-STARRS1 (PS1; Chambers et al. 2016) photometry, as part of the study by MacLeod et al. (2019, see their Table 2). The spectrum was acquired in February 2016 using the Intermediate dispersion Spectrograph and Imaging System (ISIS) mounted on the 4.2 m William Herschel Telescope (WHT) at the Roque de los Muchachos Observatory. While the 2016 spectrum showed a fainter continuum and broad Balmer line emission compared to the 2001 bright-state spectrum, the analysis of MacLeod et al. (2019) found insignificant line variability. We refer to this spectrum as the “intermediate state”.

During April–June 2021, four more spectra were obtained as part of the Black Hole Mapper program (Anderson et al., in preparation) within the ongoing fifth generation of the SDSS (SDSS-V; Kollmeier et al. 2017, Kollmeier et al., in preparation) obtained with the plate-based fiber-fed BOSS spectrograph (Smee et al. 2013) mounted on the SDSS 2.5 m telescope (Gunn et al. 2006) at the Apache Point Observatory. The four visits are part of a dedicated SDSS-V sub-program that aims to monitor previously-known quasars over timescales of weeks to years. The four SDSS-V spectra, taken within a period of ≈ 2 months, are all consistent with each other, but differ dramatically from earlier spectra, suggesting the SDSS-V spectra have captured a CLAGN event. Specifically, the quasar appeared much fainter than the previous (2001 and 2016) observations, showing an almost complete disappearance of the quasar-like blue continuum and broad $H\beta$ line emission. We refer to the state captured by these spectra as the “dim state”.

Following the identification of the spectral variability of J1628+4329, three further spectra were acquired with the FLOYDS spectrograph mounted on the 2 m Faulkes Telescope North at Haleakala, Hawaii, which is a part of the Las Cumbres Observatory network (LCO; Brown et al. 2013). The spectra were obtained ≈ 2 , 8, and 10 months after the latest dim-state SDSS-V spectrum. Surprisingly, these spectra revealed a reappearance of the blue continuum and the prominent broad $H\beta$ line emission, reverting to a state that closely resembles the 2016 intermediate-state spectrum.

Subsequent spectroscopy obtained with the ARC 3.5 m telescope (Apache Point Observatory), the Hobby-Eberly Telescope (McDonald Observatory), and the continuing SDSS-V program all confirm that J1628+4329 indeed retains its intermediate-state spectral appearance, as of 2022 May 21. The absolute flux calibration of these spectra, however, has large uncertainties, and these spectra are thus not included in our main analysis.

2.2. Multi-epoch imaging

Figure 2 shows g - and r -band photometry of J1628+4329. The photometric measurements were obtained from publicly available legacy SDSS, PS1 (Flewelling et al. 2020), and Zwicky Transient Facility (ZTF; Masci et al. 2019) data.² We also show synthetic photometry derived from each of the J1628+4329 spectra, by convolving the spectra with the respective filter curves. The PS1 photometry reveals a steady dimming, of $\Delta g \approx 1$ mag, between 2011 and 2013, consistent with the trend observed between the 2001 and the 2016 spectra. In addition, the ZTF (forced) photometry clearly confirms the rapid variations seen between the 2021 SDSS-V and LCO spectra, and clearly demonstrates that J1628+4329 became fainter by another $\Delta g \approx 1$ mag between March and June 2021, following a period of limited variability during 2018–2021. Such changes of $\Delta g \approx 1$ mag on a timescale of a few months are inconsistent with observations of typical AGNs, which require much longer timescales for similarly extreme variability to occur (see, e.g., Rumbaugh et al. 2018, and references therein).

In addition, Figure 2 displays mid-infrared photometry of J1628+4329 obtained from the Wide-field Infrared Survey Explorer (WISE; Wright et al. 2010), in the W1 and W2 bands (≈ 3.4 and $4.6 \mu\text{m}$, respectively). The WISE light curves reveal a dimming of ≈ 0.4 mag between 2011 and 2014 in both bands, and may also show hints of a slightly weaker dimming in the most recent epoch available at the time of writing, in July 2021.

2.3. Spectral analysis

We employed the PyQSOFit code (Guo et al. 2018; Shen et al. 2019) to obtain key spectral measurements of J1628+4329, in each of the various epochs observed. We first verified that the observed fluxes of the narrow [O III] $\lambda 5007$ line vary by less than $\approx 15\%$ between the different spectra (see Table 1). Considering also the relatively small angular size of J1628+4329 (compared with the apertures used; see Table 1), and the consistency between the synthetic and imaging photometry (Fig. 2), we chose to analyze the spectra without any additional scaling. In what follows, we briefly describe the key steps of the PyQSOFit fitting process.

All spectra were shifted to the rest frame and corrected for Galactic extinction using the Schlegel et al. (1998) dust maps ($A_V \approx 0.02$) and a Milky Way (MW) extinction law (see Salim & Narayanan 2020, and references therein). The faintest, most host-galaxy dominated, SDSS-V spectrum (taken in April 2021) was then decomposed to ex-

² We applied quality metrics following ZTF guidelines (https://irsa.ipac.caltech.edu/data/ZTF/docs/ztf_forced_photometry.pdf) and using procedures developed by the ALERCE team (Förster et al. 2021), which removes bad weather data and applies a color correction.

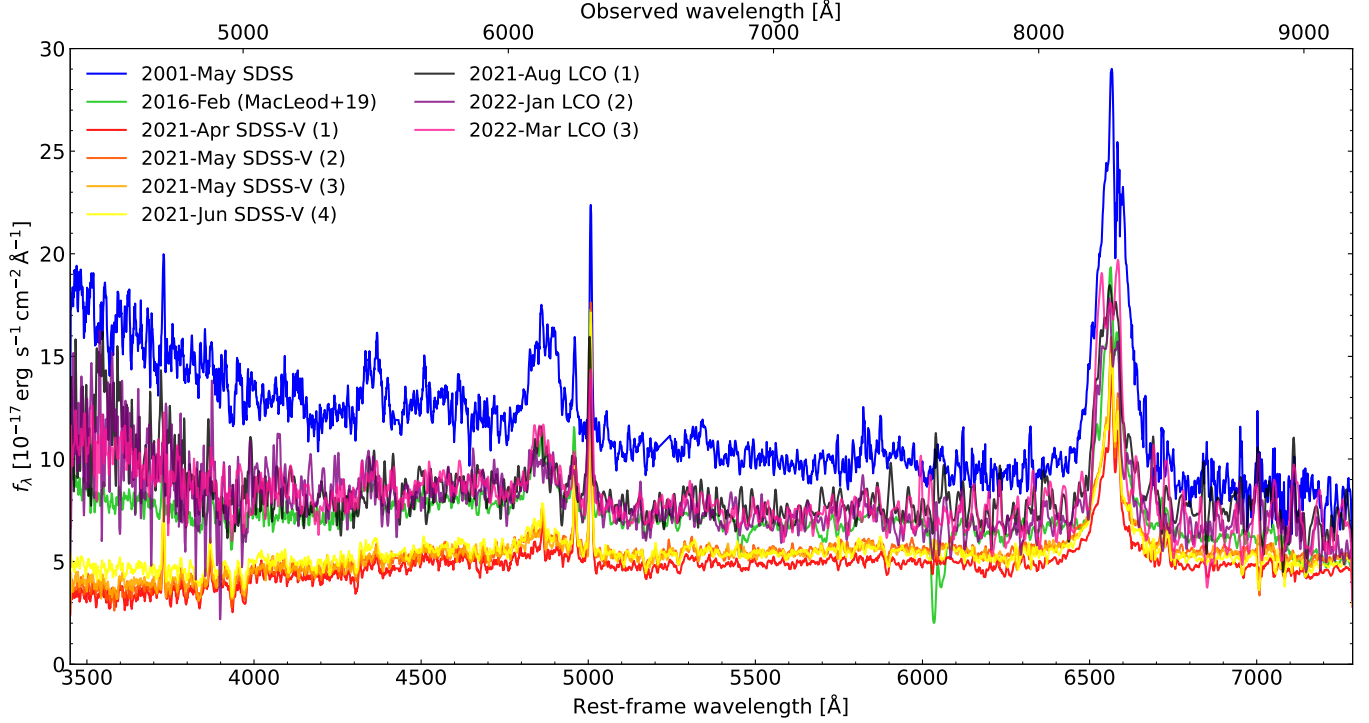


Figure 1. Multi-epoch optical spectra of J1628+4329. This AGN shows a gradual dimming of its quasar-like continuum and Balmer BELs across ~ 20 years, through the 2001 bright-state SDSS spectrum, the 2016 intermediate-state WHT spectrum (MacLeod et al. 2019), and the 2021 dim-state SDSS-V spectra. Subsequent observations performed by LCO revealed a brightening to an intermediate-state in $\lesssim 2$ months.

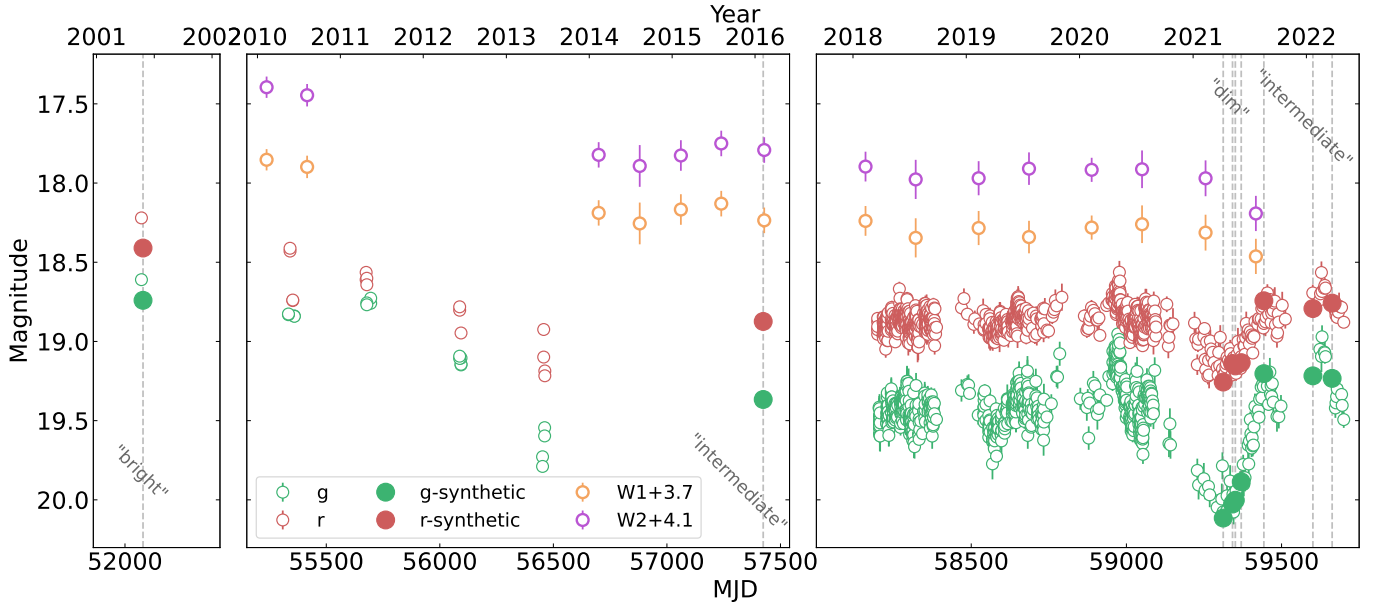


Figure 2. Optical light curves of J1628+4329 obtained from SDSS (left), Pan-STARRS (middle) and ZTF (right) imaging, in the g and r bands (open circles; see legend) over a period of two decades. For clarity, only measurements with magnitude uncertainties less than 0.1 mag are displayed. Dashed vertical lines mark the epochs of the spectra shown in Fig. 1, and the corresponding synthetic photometry is marked with filled circles. Note the fast, <2 -month transitions observed within ZTF during 2021, and the slower dimming observed within Pan-STARRS, during 2012–2014. The middle and right panels also show light curves obtained from WISE, in the $W1$ and $W2$ bands, where each data point shows the median magnitude at the given epoch. Note the vertical offset of the WISE data (for clarity; see legend).

tract the host-galaxy spectrum, relying on the template-based principal component analysis approach implemented within PyQSOFit. We then subtracted this faint-state based host spectrum from all spectra of J1628+4329. We verified that our spectral decomposition reproduces the stellar absorption features observed in the dim- and intermediate-state spectra. For the bright state, however, matching the host-galaxy features is less robust, as expected given the quasar-dominated continuum. We stress that our main analysis focuses on the intermediate-dim-intermediate transition. The continuum of the host-subtracted spectra was then modeled as a combination of a simple power-law, a Balmer continuum model, and an optical Fe II composite model. We did not add a polynomial component to the continuum modeling, as it did not significantly affect our result. We fitted all broad and narrow emission lines with one Gaussian (each), except for the broad H α line, which required two Gaussians to produce an acceptable fit. We verified that fixing the fit parameters of the narrow emission lines across all spectra did not significantly affect our results.

PyQSOFit was used to obtain the FWHM, EW and flux of the broad H α and H β emission lines, as well as the AGN-only luminosity at 5100 Å, $\lambda L_{\lambda}[5100 \text{ \AA}]$ (L_{5100} hereafter), for each of the epochs. These quantities are listed in Table 1. The uncertainties were obtained through a Monte Carlo refitting approach, using 100 realizations for each spectrum, relying on the corresponding error spectra. The best-fit spectral parameters derived from the fit of the H β complex in the (host-subtracted) ‘bright state’ spectrum and the single-epoch prescription for black-hole masses imply $\log(M_{\text{BH}}/M_{\odot}) \simeq 8.2$ (see Mejía-Restrepo et al. 2022, and references therein). Assuming an optical-to-bolometric correction of $L_{\text{bol}}/L_{5100} = 9.3$ (Shen et al. 2011) yields a mass accretion rate of $\dot{M} = L_{\text{bol}}/(\eta c^2) \simeq 0.16 M_{\odot}/\text{yr}$ (assuming $\eta = 0.1$) and an Eddington ratio of $L/L_{\text{Edd}} \equiv L_{\text{bol}}/(1.5 \times 10^{38} \times [M_{\text{BH}}/M_{\odot}]) \simeq 0.03$. The (host-subtracted) faintest SDSS-V spectrum leads to $\dot{M} \simeq 0.033 M_{\odot}/\text{yr}$ and $L/L_{\text{Edd}} \simeq 0.007$, under the same assumptions. All these quantities carry significant systematic uncertainties, of $\gtrsim 0.3$ dex.

Figure 3 presents the spectral ratio between the 2016 intermediate-state and the 2021 dim-state spectra, calculated for the host- and narrow line-subtracted spectra (i.e., the quasar-like continuum and Balmer BELs). The spectral ratio demonstrates two key aspects of the changes seen in J1628+4329: (1) the redder nature of the dim state (i.e., the ratio spectrum rises towards shorter wavelengths); and (2) the overall smooth variation of the spectral ratio across the entire wavelength range, particularly in the spectral bands adjacent to the Balmer BELs (i.e., the ratio spectrum itself shows only weak and noisy features coincident with the Balmer-lines wavelengths, and does not show features that resemble

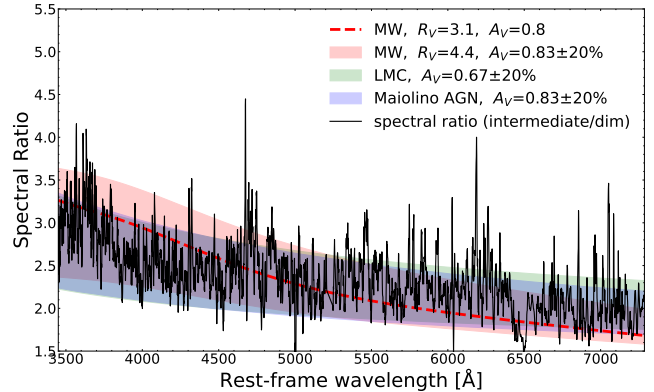


Figure 3. The spectral ratio between the 2016 intermediate-state and 2021 dim-state of J1628+4329 (black), smoothed over 7 pixels. The colored areas indicate different extinction laws: MW-like extinction with $R_V = 4.4$ and LMC-like extinction (red and green, respectively; see Salim & Narayanan 2020, and references therein), and ‘Maiolino-AGN’ extinction (blue; Maiolino et al. 2001; Li 2007). A range of possible A_V values for each extinction law is shown. Steeper extinction laws, e.g., MW-like with $R_V = 3.1$, are not consistent with the spectral ratio (see dashed line).

the broad Balmer emission profiles themselves). The implications of this figure are further explored in Section 3.

3. DISCUSSION

The dramatic variability events observed in J1628+4329 are intriguing because the source seems to transit between relatively well-defined states, over merely a few months—among the fastest CLAGN transitions seen to date (e.g., Guo et al. 2016; Trakhtenbrot et al. 2019; Ross et al. 2020). These events can be interpreted in several ways: (1) an intrinsic change in the emission from the central engine and from the BLR due to a variable accretion flow, (2) an apparent change driven by variable obscuration along the l.o.s., or (3) a more nuanced combination of the two, related to dust formation and sublimation. We discuss these possibilities below.

3.1. Variable Accretion Flow

To test the possibility of a change to the accretion flow, we consider the timescales associated with continuum variability and with the BLR response to it.

As discussed in detail in many previous studies (e.g., LaMassa et al. 2015; Stern et al. 2018), the relevant timescales for drastic changes in thin, stable accretion disks are thought to be much longer than what is observed in CLAGN transitions, even for the case of years-timescale transitions. Even more sophisticated models do not achieve coherent disk transitions on intra-year timescales (see detailed discussion in, e.g., Shen 2021, and references therein). In addition, while novel models involving magnetic flux inversion can explain rapid UV-optical flares (Scepi et al. 2021), their relevance to the dip seen in J1628+4329 is not

Table 1. Key multi-epoch spectral measurements for J1628+4329.

Date	MJD	Telescope	d^a	FWHM($H\alpha$)	EW($H\alpha$)	$F(H\alpha)/10^{-17}$	FWHM($H\beta$)	EW($H\beta$)	$F(H\beta)/10^{-17}$	$\log L_{5100}$	$F([O\text{ III}])/10^{-17}$	State
			[$''$]	[km s^{-1}]	[\AA]	[$\text{erg s}^{-1}\text{cm}^{-2}$]	[km s^{-1}]	[\AA]	[$\text{erg s}^{-1}\text{cm}^{-2}$]	[erg s^{-1}]	[$\text{erg s}^{-1}\text{cm}^{-2}$]	
2001 May 28	52057	SDSS 2.5m/SDSS	3	5011 \pm 93	425 \pm 28	2770 \pm 180	5790 \pm 190	63 \pm 2	622 \pm 17	44.0 \pm 0.005	126 $^{+5}_{-6}$	‘bright’
2016 Feb 6	57424	WHT 4.2m/ISIS	1	3750 \pm 120	337 \pm 12	1157 \pm 41	5450 \pm 160	67 \pm 1	347 \pm 7	43.7 \pm 0.004	130 \pm 3	‘intermediate’
2021 Apr 8	59312	SDSS 2.5m/BOSS	2	4130 \pm 140	423 \pm 11	681 \pm 17	6700 \pm 1200	46 \pm 5	93 \pm 10	43.3 \pm 0.006	117 $^{+3}_{-2}$	‘dim’
2021 May 8	59342	SDSS 2.5m/BOSS	2	4330 \pm 150	298 \pm 7	744 \pm 16	8800 \pm 980	71 \pm 6	178 \pm 14	43.4 \pm 0.008	122 \pm 3	
2021 May 17	59351	SDSS 2.5m/BOSS	2	4250 \pm 140	323 \pm 7	763 \pm 15	6400 \pm 1200	43 \pm 4	110 \pm 11	43.4 \pm 0.007	114 \pm 3	
2021 Jun 5	59370	SDSS 2.5m/BOSS	2	4140 \pm 110	369 \pm 7	791 \pm 16	5900 \pm 430	58 \pm 3	159 \pm 8	43.4 \pm 0.005	121 $^{+2}_{-3}$	
2021 Aug 17	59443	FTN 2m/FLOYDS	2	3920 \pm 390	247 \pm 17	1248 \pm 87	4100 \pm 1700	32 \pm 7	204 \pm 42	43.8 \pm 0.009	130 $^{+10}_{-14}$	‘intermediate’
2022 Jan 22	59601	FTN 2m/FLOYDS	2	3200 \pm 460	269 \pm 44	1070 \pm 170	4900 \pm 3600	36 \pm 13	217 \pm 81	43.8 \pm 0.01	120 $^{+27}_{-24}$	
2022 Feb 26 [*]	59636	ARC 3.5m/KOSMOS	2	3720 \pm 120	298 \pm 13		8870 \pm 460	102 \pm 4				
2022 Mar 25	59663	FTN 2m/FLOYDS	2	4040 \pm 150	321 \pm 13	1243 \pm 51	4500 \pm 300	58 \pm 3	332 \pm 16	43.8 \pm 0.006	110 $^{+5}_{-6}$	
2022 May 9 [*]	59708	SDSS 2.5m/BOSS	2	4380 \pm 370	330 \pm 30		4720 \pm 590	55 \pm 3				
2022 May 10 [*]	59709	SDSS 2.5m/BOSS	2	4170 \pm 280	397 \pm 24		4970 \pm 40	71 \pm 4				
2022 May 21 [*]	59720	HET 10m/LRS-2	b	3680 \pm 280	299 \pm 44		4820 \pm 350	61 \pm 3				

^a Aperture size: slit width or fiber diameter.

^b The spectrum was extracted from the integral field unit data cube after adopting a Gaussian point-spread function with a FWHM of $2''$. Approximately 75% of the light is enclosed in an aperture of diameter equal to the FWHM and 94% of the light is enclosed in an aperture of diameter of $2\times$ FWHM.

* These late spectra have large absolute flux calibration uncertainties and are not used for our main analysis. The corresponding FWHM and EW measurements are robust.

yet clear. J1628+4329 challenges common theoretical expectations even further, given the detailed nature of its rapid (months-timescale) transitions. Following the common calculations for other CLAGN, we note that the disk material infall timescale for J1628+4329 is ≈ 80 years (following Eq. 5 in LaMassa et al. 2015). Observationally, however, changes to the accretion flow on timescales of several months have been inferred for *some* CLAGNs events (e.g., Gezari et al. 2017; Trakhtenbrot et al. 2019). We thus cannot exclude an accretion-driven mechanism to explain J1628+4329 based solely on timescale arguments.

As for the BLR response, its timescale is expected to be dominated by the light-travel time between the ionizing source and the BLR, $t_{\text{lt}} = R_{\text{BLR}}/c$, where R_{BLR} is the characteristic radius of the BLR. Using the $R_{\text{BLR}} - L$ relation of Bentz et al. (2013) and the measured L_{5100} we infer $R_{\text{BLR}} \approx 36$ and $16 \text{ lt} - \text{days}$, for the brightest (SDSS; 2001) and faintest (SDSS-V; 2021) spectra, respectively. The corresponding light-travel timescales could thus be accommodated within the observed ≈ 60 days timescale of BLR variability of J1628+4329.

Another expectation that arises for BLR clouds moving at Keplerian velocities that are responding to continuum variations is that the typical BEL velocities would follow $\text{FWHM} \sim R_{\text{BLR}}^{-1/2} \sim L^{-1/4}$ (e.g., Barth et al. 2015; Wang et al. 2020). Between the 2001 bright state and the 2016 intermediate state, $\text{FWHM}(H\alpha)$ decreased by a factor of 1.34 ± 0.05 and $\text{FWHM}(H\beta)$ remained essentially constant (increased by a factor of 1.06 ± 0.05), while the expectation based on the

luminosity-scaling relation is for an *increase* by a factor of ≈ 1.2 . Between the 2016 intermediate state and 2021 dim state, $\text{FWHM}(H\alpha)$ and $\text{FWHM}(H\beta)$ both increased, by factors of 1.12 ± 0.04 and 1.3 ± 0.1 (respectively), consistent with a similar expectation of a uniform increase by a factor of ≈ 1.2 .

One significant challenge of the variable accretion flow hypothesis is to account for the observed spectral ratio between the intermediate and dim states, shown in Fig. 3. The lack of BLR-like features in the spectral ratio means that, for each of the Balmer BELs, the dimming factor is comparable to the one of the adjacent continuum. This result is especially surprising considering that the optical continuum is emitted from the outer parts of the accretion disk, while the broad line emission is fundamentally driven by the ionizing (>13.6 eV) radiation, which in turn originates from the inner parts of the disk. While certainly these two forms of radiation are physically linked, there is no *a-priori* reason to expect that they would scale linearly, as supported by the observed ‘bluer-when-brighter’ trend (see, e.g., Rumbaugh et al. 2018, and references therein). Specifically for J1628+4329, theoretical thin-disk spectral energy distributions that are calculated based on the observed M_{BH} and accretion rates for the intermediate-dim transition imply a variation in $L(>13.6 \text{ eV})$ by a factor of $\approx 3.6\times$, compared to the observed factor of only $\approx 2.4\times$ in the optical regime. A similar analysis for the bright-to-dim transition implies a variation by a factor of $\approx 9\times$ in $L(>13.6 \text{ eV})$, and by a factor of $\approx 5\times$ in the optical regime. Even if some of the optical continuum originates from repro-

cessed UV light in the disk or as diffuse continuum from the BLR (e.g., Chelouche et al. 2019), this cannot fully explain the interlinked continuum and line variations we observe.

Finally—and most importantly—it is challenging to explain how the variable accretion flow scenario would produce the well defined dip seen in J1628+4329 during 2021, and the (spectral) recovery back to a state essentially identical to the 2016 one.

3.2. Variation Caused by a Crossing Cloud

A variable obscuration scenario invokes an obscuring cloud intercepting the l.o.s. at the end of 2020, and then going out of the l.o.s. between 2021 June and August (Fig. 2). Another obscuring cloud, which entered our l.o.s. circa 2011, may explain the more gradual dimming between 2011-2013. This scenario is supported by the ‘dip’ in the 2021 ZTF optical light curve, and would naturally explain the similarity of the 2016 and most recent (LCO) spectra.

To quantitatively test the implications of this scenario, we applied the ‘Maiolino AGN’ extinction law (Maiolino et al. 2001; Li 2007) to the 2001 bright-state spectrum. This relatively flat extinction law has been shown to be a good description of reddening in AGNs (see, e.g., Maiolino et al. 2001; Xie et al. 2017, and references therein, but also Richards et al. 2003). For J1628+4329, this extinction law provides a good agreement between the various epochs. A similarly satisfactory agreement can also be achieved using a MW-like extinction law with $R_V = 4.4$, or an LMC-like extinction law. The top panel of Figure 4 shows representative host-galaxy and narrow-line subtracted observed spectra of J1628+4329, as well as those artificially reddened versions of the intermediate- and bright-state spectra that best match the dimmer states. Specifically, an intermediate-state spectrum reddened by $A_V \approx 0.89$ (black line) and/or a bright-state spectrum reddened by $A_V \approx 1.6$ (light gray) match the dim-state spectrum remarkably well. In addition, a bright-state spectrum reddened by $A_V \approx 0.67$ (dark gray) matches well the intermediate-state one. Assuming a MW-like dust-to-gas ratio, this analysis would imply that a dust cloud with $N_H \approx 1.6 \times 10^{21} \text{ cm}^{-2}$ has entered and exited our l.o.s. during the 2021 intermediate-dim-intermediate transition. Similarly, the bright-to-intermediate and bright-to-dim transitions would imply column densities of $N_H = 1.2$ and $2.8 \times 10^{21} \text{ cm}^{-2}$, respectively.³ The bottom panels focus on the broad Balmer emission lines ($H\alpha$, $H\beta$, $H\gamma$). The reddened spectra of the bright state show a striking similarity to the intermediate- and dim-state spectra, across the entire observed wavelength range, which strongly supports the variable obscuration interpretation. These similarities are further

demonstrated by the nearly-uniform variations in line and continuum emission seen in Fig. 3, which also shows how the several extinction curves considered here can reasonably explain the observed intermediate-to-dim spectral ratio.

The main challenge to the transient obscuration scenario relates to the observed and expected timescales. Specifically, assuming an obscurer moving at Keplerian velocities within the BH sphere of influence, the appropriate dynamical timescale is $\tau_{\text{dyn}} \approx (R_{\text{cloud}}^3/GM_{\text{BH}})^{1/2}$, where R_{cloud} is the distance of the obscuring cloud from the SMBH. Plugging in the minimal value of $R_{\text{cloud}} = R_{\text{BLR}}$ produces $\tau_{\text{dyn}} \approx 6 \text{ yr}$, a factor of ~ 35 longer than the observed shortest variability timescale of J1628+4329. A more detailed derivation that accounts for the projected l.o.s. motion of the obscurer, following LaMassa et al. (2015, see their Eq. 4), yields yet longer crossing timescales of $\gtrsim 18 \text{ yr}$. This argument becomes particularly relevant if the obscurer is part of the (clumpy) torus, i.e. if $R_{\text{cloud}} = \text{few} \times R_{\text{BLR}}$ (e.g., Risaliti et al. 2002; Koshida et al. 2014, and references therein). More generally, for an obscuring object in the AGN host galaxy to “reveal” the BLR, the obscurer has to travel a physical distance of $R_{\text{BLR}} \gtrsim 30 \text{ lt-days}$ within the < 2 months span of the fastest transition observed, and thus must move at an unreasonably high (tangential) velocity of $\gtrsim 0.5c$. Furthermore, an obscuring cloud that covers a substantial portion of the BLR would have to be of (at least) a comparable size (i.e., $\sim R_{\text{BLR}}$), which is larger by at least an order of magnitude than the expected size for clouds in the torus (Eliuzur 2008). We note that the optical variability in the spectra of some Seyfert 1.8 and 1.9 galaxies has been reported to be best explained by variable obscuration (e.g., Goodrich 1995). Those transitions, however, were identified using spectra taken several years apart, and were thus consistent with much slower obscurer velocities, of $\sim 100 - 1000 \text{ km s}^{-1}$. In addition, the presence of obscuring clouds moving in and out of the l.o.s. towards some AGNs were identified by several X-ray studies (e.g., Risaliti et al. 2005; Maiolino et al. 2010; Markowitz et al. 2014). However, in such cases the obscuring clouds must cover only the much more compact X-ray emitting region, and can thus move at lower velocities and have a smaller physical size, compared to the obscurer discussed here. In fact, the obscurers in X-ray studies are suspected to be BLR clouds (e.g., Maiolino et al. 2010), while the obscurer in the case of J1628+4329 cannot be a BLR cloud, as it is required to obscure a large part of the BLR itself.

In principle, the challenges posed by the BLR-obscuring cloud velocity and size could be addressed by a very compact BLR, or a configuration where only a small part of the BLR is visible in our l.o.s., as $v_{\text{cloud}} \propto R_{\text{cloud}} \propto R_{\text{BLR}}$. We note, however, that the observed broad $H\alpha$ strength (i.e., $L[\text{b}H\alpha]$) does not support a particularly small BLR or one with a low

³ Note, however, that many AGNs are observed to have higher gas-to-dust ratio (e.g., Maiolino et al. 2001).

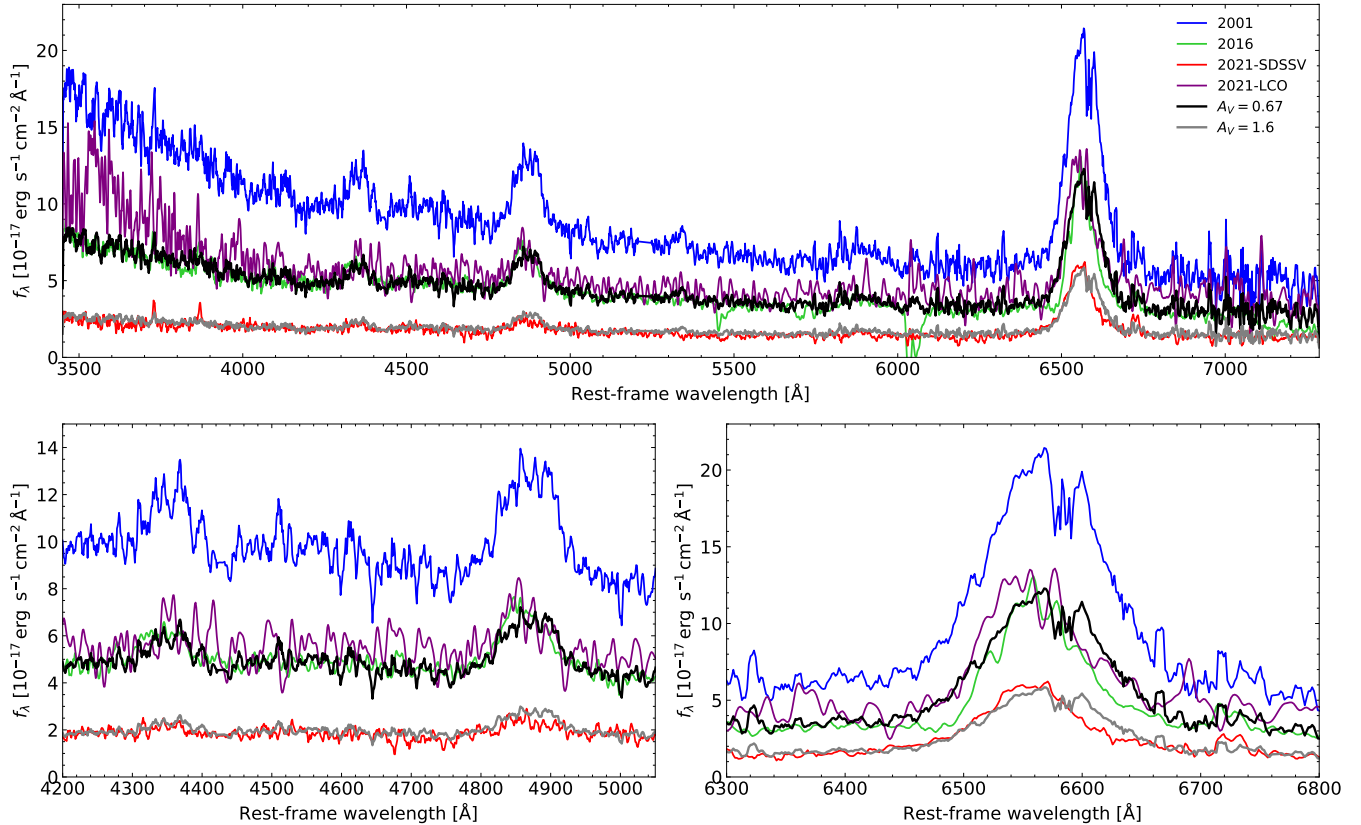


Figure 4. Representative host and narrow-line subtracted spectra of J1628+4329: 2001 bright-state (blue), 2016 intermediate-state (green), 2021 dim-state (red; SDSS-V), and 2021 intermediate-state (purple; LCO). Along those, we plot reddened spectra of the bright-state, obtained by applying the ‘Maiolino AGN’ extinction law. The appropriate A_V values were selected to best reproduce the intermediate ($A_V = 0.67$; black) and dim ($A_V = 1.6$; gray) states.

covering factor (see distributions in, e.g., [Greene & Ho 2007](#) or [Stern & Laor 2012](#) for comparison).

An additional challenge to the variable obscuration interpretation is posed by the WISE photometry (Figure 2), which shows a clear dimming of ≈ 0.4 mag in the $W1$ and $W2$ bands sometime between 2011 and 2014—as expected for the reverberation response from the dusty torus of the UV/optical accretion disk continuum variability (e.g., [Yang et al. 2020](#)). The WISE light curve also shows hints of a weaker dimming in the most recent data point, in July 2021, coincident with the recovery seen in the optical (ZTF) light curve. The interpretation of this second WISE dimming is limited by large uncertainties and the low cadence of measurements (≈ 6 months). If we assume that the dimmest WISE measurement is indeed associated with the rapid 2021 optical dip, it would be inconsistent with a variable obscuration scenario, as the WISE bands are not expected to be affected by (dust) obscuration. Thus, the limited WISE data in hand favor variable accretion as an explanation for the slow 2011 dimming, and perhaps also for the rapid 2021 event.

3.3. Rapid Dust Formation and Sublimation

The rapid changes in J1628+4329, combined with the similarity between the extinction-reddened ‘bright-state’ spectrum and the fainter spectra, raise the possibility of variable obscuration occurring on the BLR light-travel timescale, rather than dynamical timescale. In such a scenario, the rapid 2021 changes may be driven by a temporary decrease in the UV emission from the central engine, which allowed the formation of dust in the previously-sublimated, innermost parts of the dusty torus. After the UV emission reverted to its earlier state, the dust sublimated to its previous levels. Since the innermost part of the torus is thought to reside just outside the (dust-free) BLR (e.g., [Risaliti et al. 2002](#); [Koshida et al. 2014](#)), the time required for the enhanced radiation to reach the torus is only slightly longer than the BLR light-crossing time, i.e., $\text{few} \times t_{\text{IL,BLR}}$, which is consistent with the fastest variability seen in J1628+4329. The dust formation and sublimation timescales themselves are sufficiently

short for BLR-like gas densities (i.e., up to ~ 1 month for $n \simeq 10^9 \text{ cm}^{-3}$; e.g., [Draine 2009](#); [Baskin & Laor 2018](#)).⁴

A key challenge for this scenario is that it necessitates a considerable and rapid change in the UV continuum emission that did not significantly and directly affect the observed optical continuum and broad line emission, as the spectral variations are fully accounted for by varying obscuration effects (Fig. 4). This can be explained if the changes in the dust-forming UV drop and its subsequent, direct effect on the BLR emission occurred at a time unrelated to the observed spectroscopic changes. However, we cannot find direct evidence to support such a nuanced, highly interlinked, and somewhat contrived scenario within the data in hand. Moreover, the dust formation and sublimation scenario fails to explain the 2021 recovery of J1628+4329 to a spectral state essentially indistinguishable from the pre-dip one, in terms of both continuum and broad line emission (similarly to the variable accretion scenario discussed in Section 3.1). All this renders the dust formation and sublimation scenario rather challenging for explaining the rapid dimming and recovery observed during 2021.

4. CONCLUSIONS

We presented multi-epoch optical spectroscopy of J1628+4329, a ‘changing-look’ AGN identified in the recently-initiated SDSS-V project. J1628+4329 was observed in three rather distinct spectral states, with the fastest transition occurring within a timescale of less than 2 months—one of the fastest significant spectral changes observed to date.

We explored several possible explanations for the observed extreme variability of J1628+4329, driven by variations in either the accretion flow and/or the l.o.s. obscuration. The observed variability timescale appears to be consistent with changes in the radiation from the accretion flow impinging on the BLR, and also with observations of other CLAGN events driven by accretion variations (Section 3.1). This explanation is further supported by the dimming in the WISE light curve between 2011-2014 (Fig. 2).

Nonetheless, the excellent agreement between the observed dimmer spectra and the (artificially) dust-reddened bright spectrum is more naturally explained by an obscuration-driven scenario (Fig. 4). Moreover—and perhaps most importantly—the 2021 “dip” in the light curve of J1628+4329 (Fig. 2), that is also associated with a temporary transition to a dimmer and redder spectral state, followed by a recovery to a state essentially identical to that preceding the dip, is exactly what one would expect from an event driven by variable l.o.s. obscuration. This explanation, however, im-

plies exceptionally high velocity and large size for the obscurer, or else a challengingly compact BLR (Section 3.2).

The transitions observed in J1628+4329 demonstrate the richness, potential, and challenges presented by CLAGNs, as well as the importance of intra-year cadence spectroscopy for large AGN samples. The discovery of this unusual event is an early result of the SDSS-V Black Hole Mapper science program - which is spectroscopically monitoring tens of thousands of AGNs on timescales of days to years, and is thus poised to discover, monitor, and survey many more systems of this sort. Responsive, multi-wavelength follow-up observations can greatly help to determine the physical drivers of these events.

ACKNOWLEDGMENTS

We thank Aigen Li for providing us the AGN-related extinction law data (inspired by the [Li 2007](#) review).

G.Z. and B.T. acknowledge support from the European Research Council (ERC) under the European Union’s Horizon 2020 research and innovation program (grant agreement 950533) and from the Israel Science Foundation (grant 1849/19). J.R.T. acknowledges support from NSF grants CAREER-1945546, AST-2009539, and AST-2108668. We acknowledge funding from ANID - Millennium Science Initiative Program - ICN12_009 (F.E.B., L.H.G.), CATA-Basal - FB210003 (F.E.B., R.J.A.), and FONDECYT Regular - 1190818 (F.E.B.) and 1200495 (F.E.B.). R.J.A. was also supported by FONDECYT grant number 1191124. D.H. is supported by DLR grant FKZ 50OR2003. M.K. acknowledges support from DFG grant KR 3338/4-1. X.L. acknowledges support by NSF grants AST-2108162 and AST-2206499. H.I.M. acknowledges a support grant from the Joint Committee ESO-Government of Chile (ORP 028/2020). J.B. is supported by NSF grants AST-1911151 and AST-1911225, as well as by NASA grant 80NSSC19kf1639.

Funding for the Sloan Digital Sky Survey V has been provided by the Alfred P. Sloan Foundation, the Heising-Simons Foundation, and the Participating Institutions. SDSS acknowledges support and resources from the Center for High-Performance Computing at the University of Utah. The SDSS web site is www.sdss5.org.

SDSS is managed by the Astrophysical Research Consortium for the Participating Institutions of the SDSS Collaboration, including the Carnegie Institution for Science, Chilean National Time Allocation Committee (CNTAC) ratified researchers, the Gotham Participation Group, Harvard University, Heidelberg University, The Johns Hopkins University, L’Ecole polytechnique fédérale de Lausanne (EPFL), Leibniz-Institut für Astrophysik Potsdam (AIP), Max-Planck-Institut für Astronomie (MPIA Heidelberg),

⁴ However, for lower gas densities the timescales could become challengingly long, as $t \propto n^{-1}$ (e.g., [Draine 2009](#)).

Max-Planck-Institut für Extraterrestrische Physik (MPE), Nanjing University, National Astronomical Observatories of China (NAOC), New Mexico State University, The Ohio State University, Pennsylvania State University, Smithsonian Astrophysical Observatory, Space Telescope Science Institute (STScI), the Stellar Astrophysics Participation Group, Universidad Nacional Autónoma de México, University of Arizona, University of Colorado Boulder, University of Illinois at Urbana-Champaign, University of Toronto, University of Utah, University of Virginia, Yale University, and Yunnan University.

The ZTF forced-photometry service was funded under the Heising-Simons Foundation grant #12540303 (PI: Graham). The Hobby-Eberly Telescope (HET) is a joint project of the University of Texas at Austin, the Pennsylvania State University, Ludwig-Maximilians-Universität München, and Georg-August Universität Göttingen. The HET is named in honor of its principal benefactors, William P. Hobby and Robert E. Eberly.

Facilities: SDSS (SDSS and BOSS), WHT (ISIS), Las Cumbres Observatory (FLOYDS), ARC (KOSMOS), HET (LRS-2).

Software: `AstroPy` (Astropy Collaboration et al. 2018), `Matplotlib` (Hunter 2007), `NumPy` (Harris et al. 2020), `SciPy` (Virtanen et al. 2020), `PyQSOFit` (Guo et al. 2018; Shen et al. 2019)

REFERENCES

- Astropy Collaboration, Price-Whelan, A. M., Sipőcz, B. M., et al. 2018, *AJ*, 156, 123, doi: [10.3847/1538-3881/aabc4f](https://doi.org/10.3847/1538-3881/aabc4f)
- Barth, A. J., Bennert, V. N., Canalizo, G., et al. 2015, *ApJS*, 217, 26, doi: [10.1088/0067-0049/217/2/26](https://doi.org/10.1088/0067-0049/217/2/26)
- Baskin, A., & Laor, A. 2018, *MNRAS*, 474, 1970, doi: [10.1093/mnras/stx2850](https://doi.org/10.1093/mnras/stx2850)
- Bentz, M. C., Denney, K. D., Grier, C. J., et al. 2013, *ApJ*, 767, 149, doi: [10.1088/0004-637X/767/2/149](https://doi.org/10.1088/0004-637X/767/2/149)
- Brown, T. M., Baliber, N., Bianco, F. B., et al. 2013, *PASP*, 125, 1031, doi: [10.1086/673168](https://doi.org/10.1086/673168)
- Chambers, K. C., Magnier, E. A., Metcalfe, N., et al. 2016, arXiv e-prints, arXiv:1612.05560. <https://arxiv.org/abs/1612.05560>
- Chelouche, D., Pozo Nuñez, F., & Kaspi, S. 2019, *Nature Astronomy*, 3, 251, doi: [10.1038/s41550-018-0659-x](https://doi.org/10.1038/s41550-018-0659-x)
- Draine, B. T. 2009, in *Astronomical Society of the Pacific Conference Series*, Vol. 414, *Cosmic Dust - Near and Far*, ed. T. Henning, E. Grün, & J. Steinacker, 453. <https://arxiv.org/abs/0903.1658>
- Elitzur, M. 2008, *NewAR*, 52, 274, doi: [10.1016/j.newar.2008.06.010](https://doi.org/10.1016/j.newar.2008.06.010)
- Flewelling, H. A., Magnier, E. A., Chambers, K. C., et al. 2020, *ApJS*, 251, 7, doi: [10.3847/1538-4365/abb82d](https://doi.org/10.3847/1538-4365/abb82d)
- Förster, F., Cabrera-Vives, G., Castillo-Navarrete, E., et al. 2021, *AJ*, 161, 242, doi: [10.3847/1538-3881/abe9bc](https://doi.org/10.3847/1538-3881/abe9bc)
- Frederick, S., Gezari, S., Graham, M. J., et al. 2019, *ApJ*, 883, 31, doi: [10.3847/1538-4357/ab3a38](https://doi.org/10.3847/1538-4357/ab3a38)
- Gezari, S., Hung, T., Cenko, S. B., et al. 2017, *ApJ*, 835, 144, doi: [10.3847/1538-4357/835/2/144](https://doi.org/10.3847/1538-4357/835/2/144)
- Goodrich, R. W. 1995, *ApJ*, 440, 141, doi: [10.1086/175256](https://doi.org/10.1086/175256)
- Green, P. J., Pulgarin-Duque, L., Anderson, S. F., et al. 2022, *ApJ*, 933, 180, doi: [10.3847/1538-4357/ac743f](https://doi.org/10.3847/1538-4357/ac743f)
- Greene, J. E., & Ho, L. C. 2007, *ApJ*, 667, 131, doi: [10.1086/520497](https://doi.org/10.1086/520497)
- Gunn, J. E., Siegmund, W. A., Mannery, E. J., et al. 2006, *AJ*, 131, 2332, doi: [10.1086/500975](https://doi.org/10.1086/500975)
- Guo, H., Shen, Y., & Wang, S. 2018, PyQSOFit: Python code to fit the spectrum of quasars, *Astrophysics Source Code Library*. <http://ascl.net/1809.008>
- Guo, H., Malkan, M. A., Gu, M., et al. 2016, *ApJ*, 826, 186, doi: [10.3847/0004-637X/826/2/186](https://doi.org/10.3847/0004-637X/826/2/186)
- Guolo, M., Ruschel-Dutra, D., Grupe, D., et al. 2021, *MNRAS*, 508, 144, doi: [10.1093/mnras/stab2550](https://doi.org/10.1093/mnras/stab2550)
- Harris, C. R., Millman, K. J., van der Walt, S. J., et al. 2020, *Nature*, 585, 357, doi: [10.1038/s41586-020-2649-2](https://doi.org/10.1038/s41586-020-2649-2)
- Hernández-García, L., Masegosa, J., González-Martín, O., et al. 2017, *A&A*, 602, A65, doi: [10.1051/0004-6361/201730476](https://doi.org/10.1051/0004-6361/201730476)
- Hunter, J. D. 2007, *Computing in Science and Engineering*, 9, 90, doi: [10.1109/MCSE.2007.55](https://doi.org/10.1109/MCSE.2007.55)
- Kollmeier, J. A., Zasowski, G., Rix, H.-W., et al. 2017, arXiv e-prints, arXiv:1711.03234. <https://arxiv.org/abs/1711.03234>
- Koshida, S., Minezaki, T., Yoshii, Y., et al. 2014, *ApJ*, 788, 159, doi: [10.1088/0004-637X/788/2/159](https://doi.org/10.1088/0004-637X/788/2/159)
- LaMassa, S. M., Cales, S., Moran, E. C., et al. 2015, *ApJ*, 800, 144, doi: [10.1088/0004-637X/800/2/144](https://doi.org/10.1088/0004-637X/800/2/144)
- Li, A. 2007, in *Astronomical Society of the Pacific Conference Series*, Vol. 373, *The Central Engine of Active Galactic Nuclei*, ed. L. C. Ho & J. W. Wang, 561
- Liu, H., Luo, B., Brandt, W. N., et al. 2022, *ApJ*, 930, 53, doi: [10.3847/1538-4357/ac6265](https://doi.org/10.3847/1538-4357/ac6265)
- MacLeod, C. L., Green, P. J., Anderson, S. F., et al. 2019, *ApJ*, 874, 8, doi: [10.3847/1538-4357/ab05e2](https://doi.org/10.3847/1538-4357/ab05e2)
- Maiolino, R., Marconi, A., Salvati, M., et al. 2001, *A&A*, 365, 28, doi: [10.1051/0004-6361:20000177](https://doi.org/10.1051/0004-6361:20000177)
- Maiolino, R., Risaliti, G., Salvati, M., et al. 2010, *A&A*, 517, A47, doi: [10.1051/0004-6361/200913985](https://doi.org/10.1051/0004-6361/200913985)
- Markowitz, A. G., Krumpe, M., & Nikutta, R. 2014, *MNRAS*, 439, 1403, doi: [10.1093/mnras/stt2492](https://doi.org/10.1093/mnras/stt2492)
- Masci, F. J., Laher, R. R., Rusholme, B., et al. 2019, *PASP*, 131, 018003, doi: [10.1088/1538-3873/aae8ac](https://doi.org/10.1088/1538-3873/aae8ac)
- Mejía-Restrepo, J. E., Trakhtenbrot, B., Koss, M. J., et al. 2022, *ApJS*, 261, 5, doi: [10.3847/1538-4365/ac6602](https://doi.org/10.3847/1538-4365/ac6602)
- Richards, G. T., Hall, P. B., Vanden Berk, D. E., et al. 2003, *AJ*, 126, 1131, doi: [10.1086/377014](https://doi.org/10.1086/377014)
- Risaliti, G., Elvis, M., Fabbiano, G., Baldi, A., & Zezas, A. 2005, *ApJL*, 623, L93, doi: [10.1086/430252](https://doi.org/10.1086/430252)
- Risaliti, G., Elvis, M., & Nicastro, F. 2002, *ApJ*, 571, 234, doi: [10.1086/324146](https://doi.org/10.1086/324146)
- Ross, N. P., Graham, M. J., Calderone, G., et al. 2020, *MNRAS*, 498, 2339, doi: [10.1093/mnras/staa2415](https://doi.org/10.1093/mnras/staa2415)
- Ruan, J. J., Anderson, S. F., Cales, S. L., et al. 2016, *ApJ*, 826, 188, doi: [10.3847/0004-637X/826/2/188](https://doi.org/10.3847/0004-637X/826/2/188)
- Rumbaugh, N., Shen, Y., Morganson, E., et al. 2018, *ApJ*, 854, 160, doi: [10.3847/1538-4357/aaa9b6](https://doi.org/10.3847/1538-4357/aaa9b6)
- Runnoe, J. C., Cales, S., Ruan, J. J., et al. 2016, *MNRAS*, 455, 1691, doi: [10.1093/mnras/stv2385](https://doi.org/10.1093/mnras/stv2385)
- Salim, S., & Narayanan, D. 2020, *ARA&A*, 58, 529, doi: [10.1146/annurev-astro-032620-021933](https://doi.org/10.1146/annurev-astro-032620-021933)
- Scepi, N., Begelman, M. C., & Dexter, J. 2021, *MNRAS*, 502, L50, doi: [10.1093/mnras/slabb002](https://doi.org/10.1093/mnras/slabb002)
- Schlegel, D. J., Finkbeiner, D. P., & Davis, M. 1998, *ApJ*, 500, 525, doi: [10.1086/305772](https://doi.org/10.1086/305772)
- Shen, Y. 2021, *ApJ*, 921, 70, doi: [10.3847/1538-4357/ac1ce4](https://doi.org/10.3847/1538-4357/ac1ce4)
- Shen, Y., Richards, G. T., Strauss, M. A., et al. 2011, *ApJS*, 194, 45, doi: [10.1088/0067-0049/194/2/45](https://doi.org/10.1088/0067-0049/194/2/45)
- Shen, Y., Hall, P. B., Horne, K., et al. 2019, *ApJS*, 241, 34, doi: [10.3847/1538-4365/ab074f](https://doi.org/10.3847/1538-4365/ab074f)

- Sheng, Z., Wang, T., Jiang, N., et al. 2017, *ApJL*, 846, L7,
doi: [10.3847/2041-8213/aa85de](https://doi.org/10.3847/2041-8213/aa85de)
- Smee, S. A., Gunn, J. E., Uomoto, A., et al. 2013, *AJ*, 146, 32,
doi: [10.1088/0004-6256/146/2/32](https://doi.org/10.1088/0004-6256/146/2/32)
- Stern, D., McKernan, B., Graham, M. J., et al. 2018, *ApJ*, 864, 27,
doi: [10.3847/1538-4357/aac726](https://doi.org/10.3847/1538-4357/aac726)
- Stern, J., & Laor, A. 2012, *MNRAS*, 423, 600,
doi: [10.1111/j.1365-2966.2012.20901.x](https://doi.org/10.1111/j.1365-2966.2012.20901.x)
- Trakhtenbrot, B., Arcavi, I., MacLeod, C. L., et al. 2019, *ApJ*, 883,
94, doi: [10.3847/1538-4357/ab39e4](https://doi.org/10.3847/1538-4357/ab39e4)
- Virtanen, P., Gommers, R., Oliphant, T. E., et al. 2020, *Nature*
Methods, 17, 261, doi: [10.1038/s41592-019-0686-2](https://doi.org/10.1038/s41592-019-0686-2)
- Wang, S., Shen, Y., Jiang, L., et al. 2020, *ApJ*, 903, 51,
doi: [10.3847/1538-4357/abb36d](https://doi.org/10.3847/1538-4357/abb36d)
- Wright, E. L., Eisenhardt, P. R. M., Mainzer, A. K., et al. 2010, *AJ*,
140, 1868, doi: [10.1088/0004-6256/140/6/1868](https://doi.org/10.1088/0004-6256/140/6/1868)
- Xie, Y., Li, A., & Hao, L. 2017, *ApJS*, 228, 6,
doi: [10.3847/1538-4365/228/1/6](https://doi.org/10.3847/1538-4365/228/1/6)
- Yan, L., Wang, T., Jiang, N., et al. 2019, *ApJ*, 874, 44,
doi: [10.3847/1538-4357/ab074b](https://doi.org/10.3847/1538-4357/ab074b)
- Yang, Q., Wu, X.-B., Fan, X., et al. 2018, *ApJ*, 862, 109,
doi: [10.3847/1538-4357/aaca3a](https://doi.org/10.3847/1538-4357/aaca3a)
- Yang, Q., Shen, Y., Liu, X., et al. 2020, *ApJ*, 900, 58,
doi: [10.3847/1538-4357/aba59b](https://doi.org/10.3847/1538-4357/aba59b)
- York, D. G., Adelman, J., Anderson, John E., J., et al. 2000, *AJ*,
120, 1579, doi: [10.1086/301513](https://doi.org/10.1086/301513)